M.I. STOCKMAN✉
P. HEWAGEEGANA

Absolute phase effect in ultrafast optical responses of metal nanostructures

Department of Physics and Astronomy, Georgia State University, Atlanta, GA 30303, USA

ABSTRACT We predict that nonlinear ultrafast electron photoemission by strong optical fields and, potentially, other nonlinear optical responses of metal nanostructures significantly depend on the absolute (carrier–envelope) phase of excitation pulses. Strong enhancement of the local optical fields produces these responses at excitation intensities lower by order(s) of magnitude than for known systems. Prospective applications include control of ultrafast electron emission and electron injection into nanosystems. A wider class of prospective applications is the determination of the absolute phase of pulses emitted by lasers and atoms, molecules, and condensed matter at relatively low intensities.

PACS 78.67.-n; 78.47.+p; 79.60.Jv; 73.20.Mf

1 Introduction

The explosive growth of ultrafast science has recently led to understanding that nonlinear optical responses of atoms, molecules, and condensed matter to ultrashort (one or a few oscillations) pulses critically depend on the phase between the carrier oscillation of a laser pulse and its envelope [1–3], which is also called the absolute phase. Thus, the problem of the determination of the absolute phase is central for ultrafast science and has significance across disciplines, as are new physical effects that depend on and allow one to determine this phase. The previously reported measurements of the absolute phase [2, 3] used nonlinear photoelectron emission from smooth metal surfaces. Their problem is the relatively high required pulse intensity that necessitates the use of amplifiers and makes it impossible to determine the absolute phase directly from the laser oscillators and of pulses re-emitted by material objects (Raman scattering, etc.).

Motivated by the central role of the carrier–envelope phase (CEP) for a wide range of ultrafast phenomena in atomic, molecular, and condensed matter physics and their prospective applications, in this paper we propose to use metal nanostructures to enhance the ultrashort fields and make possible the determination of the absolute phase at relatively low intensities that prohibit the application of the existing methods.

✉ Fax: +1-404-651-1427, E-mail: mstockman@gsu.edu

We predict that metal nanostructures respond to an ultrashort (single or a few oscillations) laser pulse in a way that is sensitive to the CEP φ. This effect is nontrivial because relaxation times of the surface-plasmon eigenmodes responsible for the ultrafast responses of metal nanostructures are rather long, typically tens of femtoseconds in the red to near-infrared spectral region for noble metals such as silver [4]. Earlier, this long relaxation time ($\gtrsim 10–50$ fs) has allowed us to predict a possibility of the coherent control of the nanoscale femtosecond optical responses [5, 6]. Such a control has subsequently been observed in an experiment where the two-photon electron emission was nanoscale-resolved by a photoemission electron microscope (PEEM) using two-pulse optical excitation with a delay variable in ~ 100-as intervals between the two femtosecond pulses (interferometric coherent control) [7]. Recently, polarization-phase coherent control of the local energy distribution in nanosystems has been demonstrated also with the PEEM detection [8]. In these experiments complicated waveforms of the electric field vector have been used. These waveforms have been generated using the adaptive optimum control method [9].

In the above-mentioned experiments, a metal nanosystem excited by an ultrashort pulse will 'ring' for tens of oscillations. In contrast, the sensitivity to the absolute phase requires reaction within an optical cycle, i.e. on the time scale ~ 100 as. Such a sensitivity is possible since metal nanostructures also possess a very short reaction time that is inverse to their total spectral width, $\tau \sim \Delta\omega^{-1} \sim 100$ fs. This defines the minimum rise time of the nanosystem response, which potentially makes it sensitive to the absolute phase.

2 Theoretical consideration

In this paper, we consider the above-threshold (strong-field) electron emission that takes place when the energy barrier separating the metal electrons from the surrounding space (whose height is defined by the work function W_f) is slanted by a quasistationary, instantaneous[1] electric optical field $\boldsymbol{E}$ causing the electron tunneling. Such a process occurs for relatively small values of the Keldysh parameter $\gamma = (W_f/U_p)^{1/2} \lesssim 1$, where $U_p = (m/2)(eE/m\omega)^2$ is the

---

[1] We will use the term 'quasistationary' instead of the usual one in the physics of ultrastrong fields 'quasistatic' because the latter term in nanoplasmonics is reserved for the case when all sizes of the system are much less than the light wavelength.

electron quiver energy, m is the electron (effective) mass, e is the elementary charge, and ω is the optical frequency [10, 11]. The quasistationary emission is of advantage for our purpose since its dependence on the parameters of the problem, absolute phase in particular, is exponentially strong.

We follow a pioneering work of [12] and separate the electron emission process into two stages: an essentially quantum tunneling stage and the subsequent almost classical motion in free space. For the tunneling stage, the probability per unit time of tunneling [13] integrated over the electron states at the Fermi surface is given by

$$w(t_0) = 8 \frac{\hbar}{me^4} \varepsilon_F W_f^2 \nu_F \exp\left(\frac{E_W}{E(t_0)}\right) \Theta[-E(t_0)]\Theta[-A(t_0)],$$

$$E_W = \frac{4}{3e\hbar}\left(2mW_f^3\right)^{1/2},\tag{1}$$

where t_0 is the moment of the electron emission, $\Theta[\cdots]$ is the unit-step function, ε_F is the Fermi energy, ν_F is the electron state density at the Fermi surface, $E(t_0)$ is a component of the time-dependent local electric field normal to the surface of the system (our convention is that the positive value of $E(t_0)$ corresponds to the field directed away from the surface towards the free space, i.e. in the direction of an electron detector), $A(t_0)$ is the normal component of the vector potential, and the vector potential is chosen in the following gauge: $A(t) = c\int_t^\infty E(t)\,dt$, where c is the speed of light. Throughout, we set the electron charge to be $-e$. In (1), E_W is a characteristic, work-function field that defines a scale for the local field $E(t)$ that efficiently causes the photoelectron emission. Note that we neglect the effects of the electron interaction with its electrostatic image that are not expected to radically change the predicted phase dependence that originates, as shown below (see Fig. 2 and its discussion), from the corresponding phase sensitivity of the local electric fields that are the cause of the tunneling process, and themselves do not depend on it. After the tunneling, the electron velocity is given by

$$v(t) = \frac{e}{mc}A(t) + v_d, \quad v_d = -\frac{e}{mc}A(t_0),\tag{2}$$

where again t_0 is the time of emergence of an electron in the free space, which is assumed to occur by tunneling at zero velocity [12], and v_d is the drift velocity, which is the asymptotic (final) velocity of the electron reached after the end of the excitation pulse. Note that the $\Theta[-E(t_0)]$ factor in (1) ensures that the electron initially accelerates away from the metal surface, and $\Theta[-A(t_0)]$ guarantees that the drift velocity of the electron is likewise directed from the metal surface into the free space. An excitation pulse generates a bunch of electrons that drift away from the metal surface generating a current density

$$j = -env_d \int_{-\infty}^{\infty} w(t)\,dt,\tag{3}$$

where n is the density of electrons in the emitting layer, and v_d is the component of the drift velocity normal to the metal surface and directed away from the metal.

From the previous work, we know that only nonlinear processes are coherently controllable when integrated over
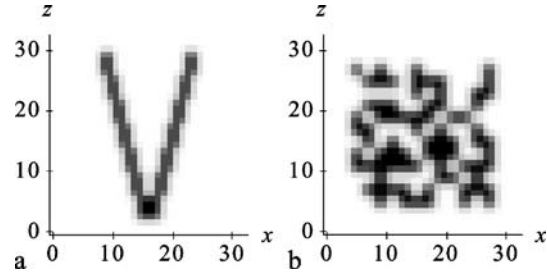

FIGURE 1 The geometry of the nanosystems in the cross section through the x–z plane of symmetry: V-shape (**a**) and random planar composite (**b**). The units in x and z axes are nm. The thickness of both the systems in the y direction is set to be 4 nm

time [5, 6]. We have chosen the strong-field (above-threshold) photoemission because it is a highly nonlinear optical process and as such is the most sensitive to the absolute phase. The electron photoemission current as given by (1)–(3) exponentially depends on the time kinetics of the local optical electric field $E(t)$ at every point of the metal nanosystem. To find this field in a general case for a strong excitation field E_0 would have been an extremely complicated, unrealistic task. However, there are the following two properties of the metal nanosystems that make an approximate solution possible.

(i) In the optical spectral region, the dielectric permittivity ε of noble metals is very large and negative, $\varepsilon \ll -1$ [14]. Correspondingly, the normal field, which causes the photoemission, can be strong enough outside the metal to slant the work-function barrier sufficiently to produce the photoemission, but inside the metal this local field may still be small enough to be treated by linear response theory.

(ii) To have the Keldysh parameter γ [10, 11] sufficiently small for moderate light intensities, we consider a near-infrared spectral region. In this case, the quality factor of the metal plasmon resonances is high enough, i.e. $\operatorname{Im}\varepsilon \ll -\operatorname{Re}\varepsilon$. This implies that the normal field in the metal is almost real and opposite in sign to (out of phase with) the normal field outside. Because for the emission the outside field should be directed outward from the metal, the inside field is necessarily directed inward and cannot cause the photoemission. Consequently, the above-threshold (strong-field) photoemission under such conditions can only occur from a very thin (on order of the Debye or Thomas–Fermi length, which is on a tenth of a nanometer scale for metals) layer at the surface where the local field $E(t)$ is the exterior (outside of the metal) optical field at the surface.

3 Numerical examples

In accord with the above-given arguments, we use a previously developed linear-response Green-function numerical approach [6] yielding the local field at each spatio-temporal point, $E(r, t)$. The current density $j(r)$ is computed by a numerical integration over the time in (3) at each spatial point. For our numerical computations, we choose silver as the metal because it has the smallest optical losses of any natural metal in the visible and infrared spectrum [14]. We consider two planar nanosystems whose geometry is illustrated in Fig. 1: V-shape [panel (a)] and random planar composite (RPC) [panel (b)]. We choose a coordinate
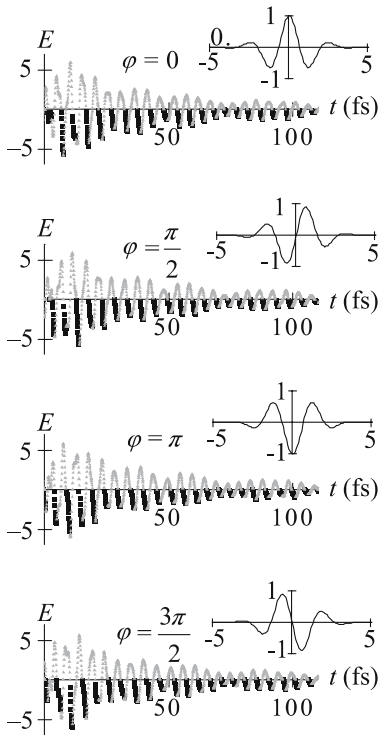
FIGURE 2 Temporal dependences of local electric optical field (the *y* component, in units of excitation field E_0) at the apex of V-shape for values of absolute phase φ indicated in panels. The *black squares* denote the temporal points contributing to the current in (1) where the Θ function arguments are positive; the *gray triangles* denote the points that do not contribute to the photocurrent. The corresponding excitation pulses are shown in the *insets* at the *upper right corners* of the corresponding panels

FIGURE 3 Distributions of photoelectron current density $j(\boldsymbol{r})$ over surface of V-shape computed from (3) shown by gray-level density plot for the values of absolute phase φ indicated. The highest current is shown by the *black* rectangles and corresponds to the relative value shown at the *top* denoted 'max'. The geometry of the system is shown in the plots by *light gray shadows* superimposed on the current distribution. The panel (**a**) corresponds to the minimum and (**b**) to the maximum current depending on φ

FIGURE 4 Total current J as a function of absolute phase φ for (**a**) V-shape at $\hbar\omega_0 = 1.55$ eV and (**b**) RPC at $\hbar\omega_0 = 1.25$ eV. The current $J(\varphi)$ is plotted in relative units where its maximum is ascribed a value of 1

frame in such a way that the nanosystem is in the *x–z* plane with the *z* polarization of the excitation pulse; the V-shape axis of symmetry is oriented along the *z* axis. The positive *y*-axis direction is set toward the electron detectors, so it is the *y* component of the local field to cause the photoemission.

The physical basis of the absolute-phase dependence of the optical effects in nanostructured metals can be traced in Fig. 2 where we display the local optical fields at the apex of the V-shape. The corresponding single-oscillation excitation pulses are shown in the insets; the medium (carrier) frequency $\hbar\omega_0 = 1.55$ eV corresponds to the radiation of a Ti:sapphire laser. The most important feature is the evident dependence of the first few oscillations of the local fields on the absolute phase: each of the shape, magnitude, and darkness of the points in the graphs, which describes the ability of the field to contribute to the photocurrent, change with φ. The change of the sign of the current (corresponding to the change from the black squares to gray triangles in the graphs) does not occur exactly at the minima of E that would have been the case if these oscillations were purely harmonic. This and the non-harmonic shape of the early oscillations indicate that many surface-plasmon eigenmodes contribute to these oscillations, which is a major factor determining the absolute-phase sensitivity. This sensitivity is due to the large bandwidth of the optical response of metals. Note, that in contrast, the later oscillations (fifth and subsequent in the figure) are not φ-sensitive.
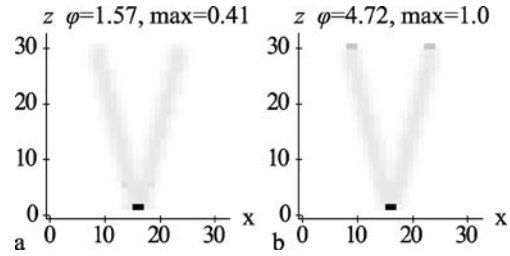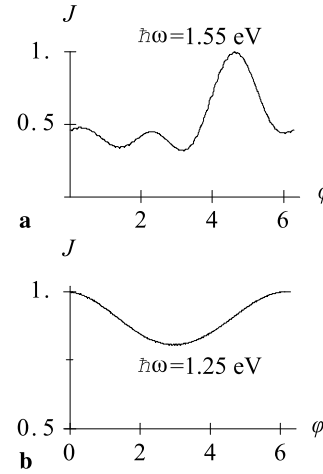
In contrast to linear-response fields, the tunneling current exponentially depends on the scale of the local optical fields (cf. (1)). In our computations, for the sake of definiteness, we choose the excitation field to be such that the maximum local field $E_m = \max[-E(\boldsymbol{r}, t)]$ yields the maximum exponential in (1) equal to $\exp(-E_W/E_m) = 10^{-3}$. The distributions of the photoelectron current density over the surface of a V-shape are shown in Fig. 3. Here, and below, we are only interested in the phase dependence of the current. Therefore, the current dependence is given relative to its global maximum in time and space (which is arbitrarily ascribed a value of 1). From this figure, it is evident that, irrespectively of φ, the maximum photocurrent density is concentrated at a hot spot at the apex (tip) with weak emitting spots elsewhere on the surface. Importantly, the magnitude of the current changes by 60%, which is a very strong absolute-phase dependence.

Integrating $j(\boldsymbol{r})$ over the surface of the V-shape, we obtain and show in Fig. 4a the total current as a function of the absolute phase, $J(\varphi)$. We see that this function has multiple maxima, but one of these maxima, at $\varphi \approx 3\pi/2$, dominates. Given the large amplitude of the φ-dependence, this maximum is quite suitable for the calibration of the absolute phase. To understand the physical origin of this maximum and generally the absolute phase sensitivity of the photoemission, let us compare with Fig. 2. Only at this value of $\varphi = 3\pi/2$ does the
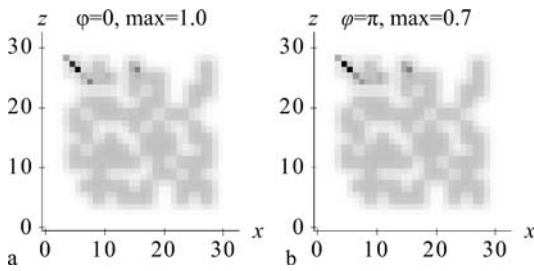
FIGURE 5 Same as in Fig. 3 but for RPC

minimum (negative maximum) of the field occur at $A(t) < 0$ (as described by the black squares in contrast to the gray triangles). This implies that electrons, which are most efficiently emitted at the negative field maximum, drift toward the free space and create the observable current, in contrast to the other φ values illustrated in Fig. 2.

While it is possible to find the absolute phase from the electron emission at smooth surfaces [2, 3], the advantage of using a metal nanostructured system for this purpose is a relatively large value of the local field, enhanced by a factor of ≈ 5 (cf. Fig. 2), which allows one to observe the same photocurrent at the excitation intensities ≈ 25 times lower than for a flat metal surface. As an example, in our case the peak instantaneous intensity of the local field can be estimated to be 1.2×10^{14} W/cm^2 corresponding to the Keldysh parameter that is reasonably small, $\gamma \approx 0.9$. At the same time, the required peak intensity of the excitation radiation is much smaller, 4.8×10^{12} W/cm^2. Note that the ponderomotive acceleration of an electron by the local field causes it to acquire energy up to $E_{max} = 3U_p$ as shown earlier [15]. For a local intensity of 4.8×10^{12} W/cm^2, this maximum energy is $E_{max} = 21$ eV.

There has been a recent theoretical publication that predicted CEP sensitivity of a multi-photon electron emission from smooth metal surfaces with propagating surface-plasmon polaritons [16]. Generally, the local fields of the propagating surface-plasmon polaritons considered in that paper are smaller than the fields of the localized surface plasmons that we consider in this work. Nevertheless, in [16], the ponderomotive forces have accelerated electrons to energies on order of $0.1-1$ keV, which are one to two orders of magnitude greater than in the present work.

Now consider the RPC nanosystem whose geometry is shown in Fig. 1b, where we have carried out computations for $\hbar\omega_0 = 1.25$ eV radiation, close to the communications range. They show that the peak amplitude of the local fields is in this case significantly higher, $E_m \approx 20$, which corresponds to the peak local-field intensity enhanced by a factor of ≈ 400 (data not shown). Similar to the case of a V-shape, for the RPC the spatial distributions of the emission current are not significantly dependent on φ, as the data shown in Fig. 5 show. The corresponding dependence of the total photocurrent on the absolute phase shown in Fig. 4b shows high enough modulation ($\approx 30\%$) that is also quite suitable for the absolute-phase determination. Note that the maxima in Fig. 4a and b are reached at different phases φ, which certainly is related to different proximities to the corresponding surface-plasmon resonances.

4   Conclusions

To conclude, we have investigated strong optical-field emission of electrons from a metal nanostructure excited by extremely short (one optical oscillation) pulses. This photoemission is shown to be highly sensitive to the absolute (carrier–envelope) phase of these pulses. The local optical-field enhancement taking place in metal plasmonic nanostructures results in this effect occurring at an order of magnitude or more lower intensities than in other systems, including flat metal surfaces. These results have a two-pronged significance. First, this effect opens up new possibilities in the physics of a wide class of enhanced optical phenomena and their spatio-temporal control on the fastest possible temporal scale ~ 100 as, within single or a few optical oscillations. There are prospective direct applications of this effect in the ultrafast nanoscale optoelectronics, e.g. for attosecond, phase-controlled injection of carriers from metal to other systems: molecular, metal, and semiconductor. Even wider class applications are foreseen as a tool in the study of ultrafast phenomena in other systems. This includes, in particular, the absolute-phase determination of relatively low-intensity ultrashort laser pulses and those of optical radiation emitted by various chemical and biological objects including atoms, molecules, clusters, and condensed matter.

REFERENCES

1 R. Kienberger, E. Goulielmakis, M. Uiberacker, A. Baltuska, V. Yakovlev, F. Bammer, A. Scrinzi, T. Westerwalbesloh, U. Kleineberg, U. Heinzmann, M. Drescher, F. Krausz, Nature **427**, 817 (2004)
2 C. Lemell, X.-M. Tong, F. Krausz, J. Burgdoerfer, Phys. Rev. Lett. **90**, 076403 (2003)
3 A. Apolonski, P. Dombi, G.G. Paulus, M. Kakehata, R. Holzwarth, T. Udem, C. Lemell, K. Torizuka, J. Burgdörfer, T.W. Hänsch, F. Krausz, Phys. Rev. Lett. **92**, 073902 (2004)
4 F. Stietz, J. Bosbach, T. Wenzel, T. Vartanyan, A. Goldmann, F. Trägger, Phys. Rev. Lett. **84**, 5644 (2000)
5 M.I. Stockman, S.V. Faleev, D.J. Bergman, Phys. Rev. Lett. **88**, 067402 (2002)
6 M.I. Stockman, D.J. Bergman, T. Kobayashi, Phys. Rev. B **69**, 054202 (2004)
7 A. Kubo, K. Onda, H. Petek, Z. Sun, Y.S. Jung, H.K. Kim, Nano Lett. **5**, 1123 (2005)
8 M. Aeschlimann, M. Bauer, D. Bayer, T. Brixner, F.J. Garcia de Abajo, W. Pfeiffer, M. Rohmer, C. Spindler, F. Steeb, Nature **446**, 301 (2007)
9 H. Rabitz, R. de Vivie-Riedle, M. Motzkus, K. Kompa, Science **288**, 824 (2000)
10 L.V. Keldysh, J. Exp. Theor. Phys. (USSR) **47**, 1945 (1964)
11 L.V. Keldysh, J. Exp. Theor. Phys. (USSR) **20**, 1307 (1965)
12 P.B. Corkum, N.H. Burnett, F. Brunel, Phys. Rev. Lett. **62**, 1259 (1989)
13 L.D. Landau, E.M. Lifshitz, *Quantum Mechanics: Non-Relativistic Theory* (Pergamon, Oxford, New York, 1965)
14 P.B. Johnson, R.W. Christy, Phys. Rev. B **6**, 4370 (1972)
15 J. Kupersztych, P. Monchicourt, M. Raynaud, Phys. Rev. Lett. **86**, 5180 (2001)
16 S.E. Irvine, P. Dombi, G. Farkas, A.Y. Elezzabi, Phys. Rev. Lett. **97**, 1468011 (2006)